Proceedings of the
International Conference on Mechanical Engineering 2011
(ICME2011) 18-20 December 2011, Dhaka, Bangladesh

ICME11-RT-022

INFLUENCE OF SUBSTITUTION OF TRANSITION METAL ION ON STRUCTURAL AND MAGNETIC PROPERTIES OF Mn-Zn FERRITES

F. Alam[1] and A. K. M. Akther Hossain[2]

[1] School of Engineering and Computer Science, Independent University, Bangladesh, Dhaka-1229
[2] Department of Physics, Bangladesh University of Engineering and Technology, Bangladesh

ABSTRACT

A series of composition $Mn_{0.50}Zn_{0.50-x}Cu_xFe_2O_4$ (where x = 0.00- 0.40) have been prepared to investigate the influence of transition metal ion, Cu^{2+} on their structural and magnetic properties. The X-ray diffraction analysis confirmed the formation of single phase cubic spinel structure. The lattice parameter of the compositions decreases with Cu^{2+} content. The bulk density (ρ_B) was found to decrease with increase in Cu^{2+} content. The grain size and initial permeability, $\mu_i^{/}$, also decrease with substitution of Cu^{2+}, where as the relaxation frequency (f_r), porosity. The saturation magnetization, M_s, decreases for x = 0.10 beyond that value of x, M_s increases. The B-H loops were measured at room temperature. The coercivity H_c, and hysteresis losses are found to increase. Possible explanations for obsrved influence of Cu^{2+} on the structural and magnetic properties of MnZnCu ferrites are discussed.

Keywords: Mn-Zn Ferrites, Auto Combustion, Initial Permeability, Saturation Magnetization And Coercivity.

1. INTRODUCTION

Ferrites have been used as high frequency soft magnetic materials due to their high resistivity and high permeability [1]. Of all ferrites, the Mn-Zn ferrites are of the greatest practical importance nowadays [2-3]. The reason for the superiority over the other ferrites, such as Ni-Zn ferrite, is the higher saturation magnetization, the lower losses, and a relatively high Néel temperature. This is due to the fact that the Mn^{2+} has 5 Bohr magnetons (μ_B) while the Ni^{2+} has only $2.3\mu_B$. The Mn-Zn ferrites has been widely used in electronic devices such as transformers, choke coil, thin-film read heads, and microwave acoustic devices up to 5×10^8 Hz, owing to its high magnetization, high resistivity, and low eddy-current losses. During the last few decades, there has been a growing interest in the study of the magnetic behavior and magnetic structure of mixed ferrite due to its fascinating properties and interesting technological applications [4-8]. The substitution of magnetic/nonmagnetic ions has shown a tremendous effect in controlling the magnetic, structural, and electrical properties. The magnetic oxide with spinel structure seems to be particularly attractive, as they allow a variety of magnetic disorders and frustrations to be introduced [9]. In spinel lattice AB_2O_4, the anions (O^{-2} ions) form cubic close packing, in which the interstices are occupied by tetrahedral (form the A-site and octahedral (form the B-sites) coordinated cations. In such magnetic oxide materials the competition between ferromagnetic and antiferromagnetic super-exchange interactions occurs between the spins of intersublattice and intrasublattices. In general, in spinel oxides intrasublattice interactions are weaker than the intersublattice interactions.

Microstructure, magnetic and electrical properties of Mn-Zn mixed ferrites depend on the method of preparation, sintering temperatures and the doping concentrations. Due to substitution of various cations, spinel type lattice may either compress or expand, hence there is a modification of A-B interaction, and also there is cation redistribution in A-site and B-sites that produce samples with various interesting properties.

2. EXPERIMENTAL DETAILS

The powders of $Mn_{0.50}Zn_{0.50-x}Cu_xFe_2O_4$ with x = 0.00, 0.10, 0.20, 0.30 and 0.40 were prepared through combustion method. Stoichiometric amounts of commercially available $MnCl_2.4H_2O$, $Cu(NO_3)_2.3H_2O$, $Zn(NO_3)_2.6H_2O$, $Fe(NO_3)_3.9H_2O$ were dissolved in ethanol. Then the solution was heated at 343K to transform into gel, the dried gel burnt out to form fluffy loose powders. Then the resultant powders were calcined at 973K for 5h and then pressed uniaxially into disk-shaped (about 0.01 mm outer diameter, 0.002-0.003 m thickness) and toroid-shaped (about 0.01 m outer diameters, 0.005 m inner diameter, and 0.003 m thickness) samples. The samples were sintered at 1473K, 1503K and 1523K for 5 h in air. The temperature ramps were $0.16Ks^{-1}$ for heating and $0.08 Ks^{-1}$ for cooling.

Microstructural properties were investigated with a

high-resolution optical microscope. The bulk density was measured by ρ_B = M/V where M is the mass of the sample and V is the volume. Average grain sizes (grain diameter) of the samples were determined from optical micrographs by linear intercept technique [10].

The frequency characteristics of Mn-Zn ferrite samples i.e. the initial permeability spectra were investigated using an Agilent Impedance Analyzer (model no. 4192A). The complex permeability measurements on toroid-shaped specimens have been carried out at room temperature on all the samples in the frequency range 10^3Hz-10^8Hz. The values of the measured parameters obtained as a function of frequency and the real part (μ_i') of the complex permeability have been calculated using the following relations: $\mu_i' = L_s/L_o$, where L_s is the self inductance of the sample core and $L_o = (\mu_o N^2 h/2\pi)\, Ln(r_o/r_i)$ is derived geometrically. Where L_o is the inductance of the winding coil without the sample core, N is the number of turns of the coil (N = 5), h is the thickness, r_o is the outer radius and r_i is the inner radius of the toroidal specimen. The relative quality factor was calculated from the relation: $Q = \mu_i'/\tan\delta$, where $\tan\delta$ is the loss factor.

3. RESULTS AND DISCUSSION

3.1 Lattice parameter, density and porosity of the samples

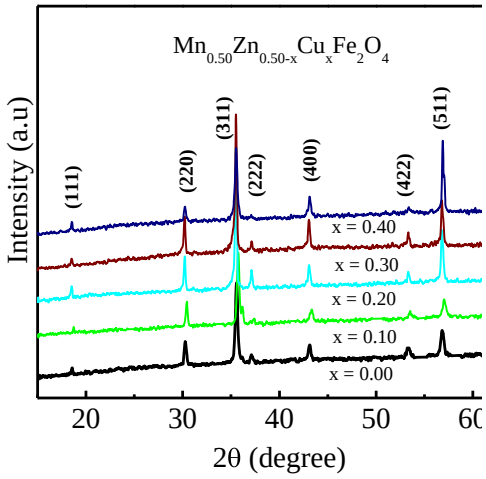

Fig 1. The XRD patterns for $Mn_{0.50}Zn_{0.50-x}\ Cu_xFe_2O_4$

Figure 1 shows the X-ray diffraction (XRD) pattern of various $Mn_{0.50}Zn_{0.50-x}Cu_xFe_2O_4$ (with x = 0.00, 0.10, 0.20, 0.30 and 0.40) sintered at 1473K. The observed diffraction peaks comply with the reported values thus confirming the formation of single phase cubic spinel structure and no unreacted constituents were present in these samples [11]. The exact values of lattice constant were estimated from the extrapolation of the lines to $F(\theta) = 0$ or $\theta = 90°$. The variation of lattice parameter 'a_0' as a function of Cu content is shown in Figure 2. It is seen from the figure that the lattice parameter decreases with increasing *Cu* content. This can be attributed that the ionic radius of Cu^{2+} ions ($7.2x10^{-09}$m) is smaller than that of Zn^{2+} ions ($7.4x10^{-09}$m) [12]. When the smaller Cu ions enter the lattice, the unit cell compressed while preserving the over all cubic symmetry. It is observed that the bulk density decreases with increasing Cu substitution as shown in figure 3. This phenomenon could be explained in terms of the atomic weight. The atomic weight of Zn is greater than that of Cu [13]. On the other hand, porosity of the sample increases with increasing Cu content resulting from discontinuous grain growth.

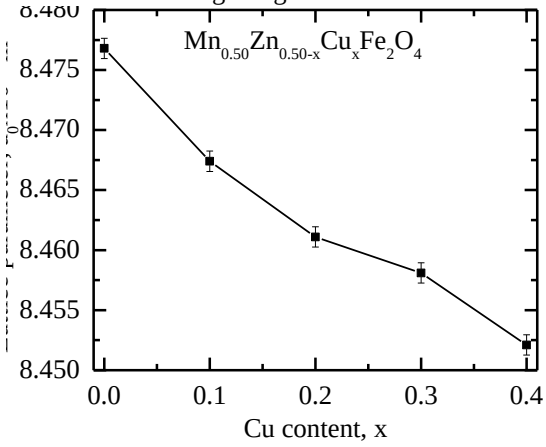

Fig 2. Variation of lattice parameter with Cu content of $Mn_{0.50}Zn_{0.50-x}Cu_xFe_2O_4$.

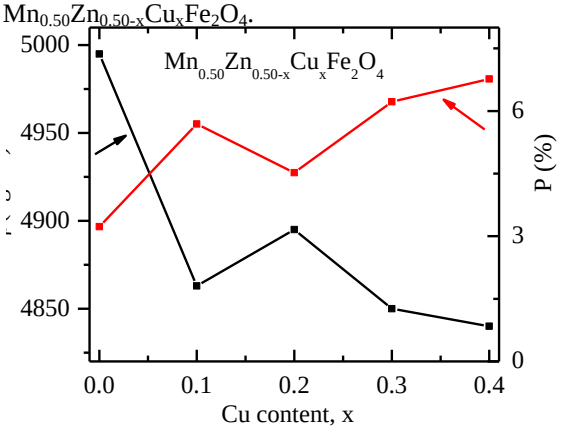

Fig 3. Variation of Density and porosity of $Mn_{0.50}Zn_{0.50-x}Cu_xFe_2O_4$ with Cu content sintered at 1473K

3.2 B-H loops of $Mn_{0.50}Zn_{0.50-x}Cu_xFe_2O_4$

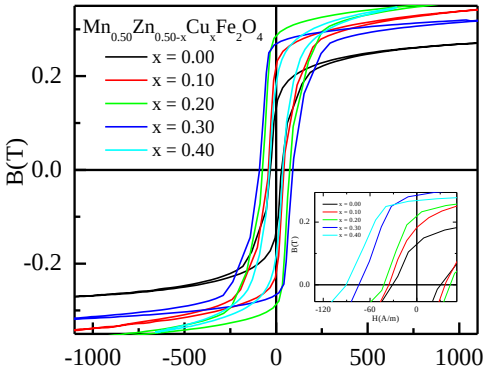

Fig 4. The B-H loops for $Mn_{0.50}Zn_{0.50-x}\ Cu_xFe_2O_4$ with x = 0.00, 0.10, 0.20, 0.30 and 0.40.

The B-H loops of the Mn-Zn-Cu ferrite were measured

at room temperature at constant frequency f = 1000 Hz as shown in Figure 4 It is observed that H_c increases with the increase in Cu^{2+}. Increase in H_c with increase in Cu may be due to the increase in magnetocrystalline anisotropy . It is well known that all these properties are extrinsic, which depend on the grain size, intra- and inter-granular porosity. Intragranular porosity occurs for higher content of Cu, which affects the magnetic properties. The area within the loop is directly related to the hysteresis loss. It is seen from the figure 4 that the loop area of B-H curve increases significantly, here by increases the hysteresis loss.

3.3 Complex initial permeability

The real part of complex initial permeability of $Mn_{0.50}Zn_{0.50-x}Cu_xFe_2O_4$ has the highest value when no copper is substituted. The permeability decreases with increasing Cu content in $Mn_{0.50}Zn_{0.50-x}Cu_xFe_2O_4$ as shown in figure 5. The composition shows resonance frequency; with real part $\mu_i^{/}$ decreases drastically at high frequency above 5MHz (depending on composition and sintering temperatures). But we observed that for $Mn_{0.50}Zn_{0.30}Cu_{0.20}Fe_2O_4$, $\mu_i^{/}$ was found to be maximum at 1473K. If the sintering temperature is higher than that of optimum, $\mu_i^{/}$ decreases as shown in figure 6. It is possible that the sample sintered at higher temperature increases the number of pores within the grain. The pores acts as pinning sites for the domain wall movement. Consequently, domain wall motion is restricted and this limits the rate of growth of permeability.

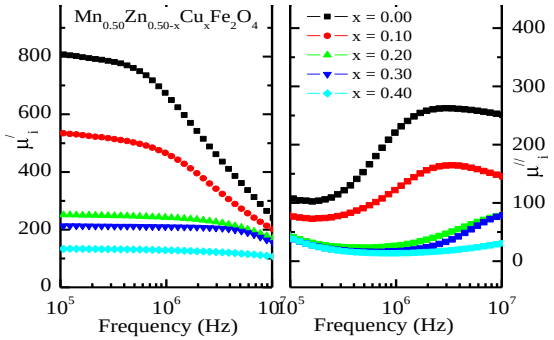

Fig 5. The frequency dependence of initial permeability of various $Mn_{0.50}Zn_{0.50-x}Cu_xFe_2O_4$ sintered at 1473K for 5h.

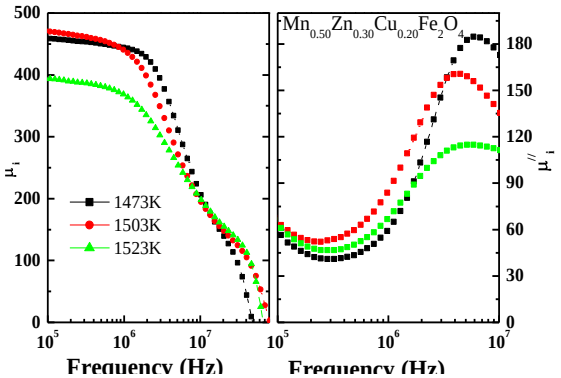

Fig 6. The variation of complex initial permeability with frequency of $Mn_{0.50}Zn_{0.30}Cu_{0.20}Fe_2O_4$ sintered at different temperatures.

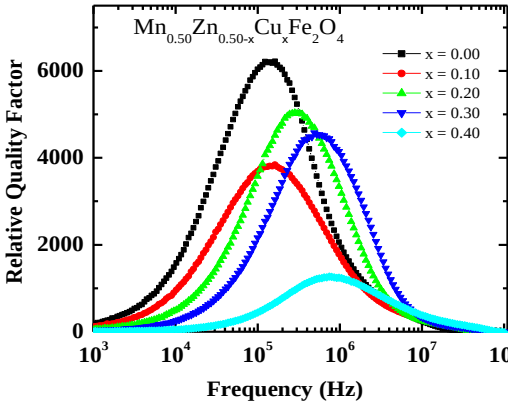

Fig 7. The frequency dependent relative quality factor in $Mn_{0.50}Zn_{0.50-x}Cu_xFe_2O_4$ sintered at 1473K.

3.4 Relative quality factor

The variation of relative quality factor with frequency for various doping concentration of the composition sintered at 1473K is shown in figure 7. The loss is due to lag of motion of domain walls with respect to the applied alternating magnetic field and is attributed to imperfections in the lattice [14, 15]. The sample sintered at 1503K has highest Q value while at 1523K it is the lowest as shown in figure 8.

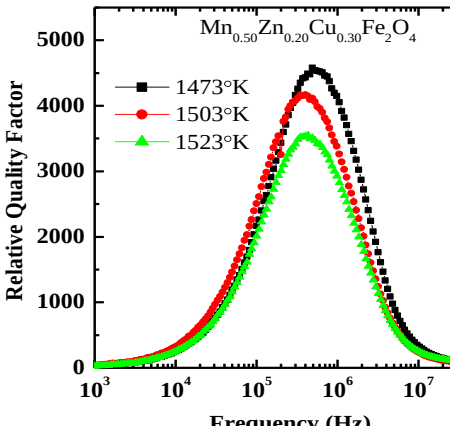

Fig 8. The frequency dependent relative quality factor of $Mn_{0.50}Zn_{0.20}Cu_{0.30}Fe_2O_4$ at different sintering temperature.

4. CONCLUSION

The lattice parameter and density of polycrystalline $Mn_{0.50}Zn_{0.50-x}Cu_xFe_2O_4$ decreases with increasing Cu substitution. With the increase of sintering temperature, the $\mu_i^{/}$ and Q of these ferrites increase up to 1503K but above 1503K there is a decrease of these values. The $\mu_i^{/}$ of the samples strongly depends on average grain size and porosity. B-H loop study reveals that with substitution of Cu content in mn-Zn ferrite enhances the hardness of the material.

5. REFERENCES

1. Smit, J. and Wijn, H. P. J., 1959, *Ferrites*, Philips, Holland.
2. Snoek, J. L., 1949, *New Developments in Ferromagnetic Materials*, Elsevier Publishing Company, Inc., Newyork.
3. Smit, J. and Wijn, H. P. J., 1954, *Advances in*

Electronics and Electron Phys., 6:69-136.
4. Yafet, Y. and Kittel, C., 1952, "Antiferromagnetic Arrangements in Ferrites", Phys. Rev., 87(2):290-294.
5. Khan, D. C., Mishra, M. and Das, A. R., 1982, "Structure and Magnetization studies of Ti-substituted $Ni_{0.3}Zn_{0.7}Fe_2O_4$", J. Appl. Phys., 53:2722.
6. Das, A. R., Ananthan, V. S. and Khan, D. C., 1985,
7. "Lattice parameter variation and magnetization studies on titanium-, zirconium-, and tin- substituted nickel-zinc ferrites", J. Appl. Phys., 57:4189.
8. Brand, R. A., Georges-Gibert, H., Hubsch, J. and Heller, I. A., 1985 "Ferrimagnetic to spin glass transition in the mixed spinel $Mg_{1+t}Fe_{2-2t}Ti_tO_4$: a Mossbauer and DC susceptibility study", J. Phys. F: Met. Phys., 15:1987.
9. Gavoille, G., Hubsch, J. and Mirebeau, I., 1997, "A magnetization study of the frustrated spinel compound $Mg_{1.55}Fe_{0.9}Ti_{0.55}O_4$", J. Magn. Magn. Mater., 171:291.
10. Dormann, J. L. and Nogues, M., 1990, "Magnetic structures in substituted ferrites", J. Phys.: Condens. Matter, 2:1223.
11. Mendelson, M. I., 1969, "Average Grain size in Polycrystalline Ceramics", J. Am. Ceram. Soc., 52(8):443.
12. Rath, C., Anand, S., Das, R. P., Sahu, K. K., Kulkarni, S. D., Date, S. K., Mishra, N. C., 2002, "Dependence on cation distribution of particle size, lattice parameter, and magnetic properties in nanosize Mn-Zn ferrite", J. Appl. Phys., 91(4):2211.
13. Shanon, R. D., 1967, *Acta Crystallogr.*, A32:751.
14. Kittel, C., 1996, *Introduction to Solid State Physics*, Seventh ed., Wiley, Singapore.
15. Chauhan, B. S., Kumar, R., Jadhav, K. M., Singh, M., 2004, "Magnetic study of substituted Mg-Mn ferrite synthesized by citrate precursor method", J. Magn. Magn. Mater., 283:71.

6. NOMENCLATURE

Symbol	Meaning	Unit
ρ	Density	(Kg/m^3)
T	Temperature	(K)
f	Frequency	(Hz)
a_0	Lattice constant	(m)
Q	Relative Quality Factor	-
$\mu_i^{/}$	Real Part of Initial Permeability	-
$\mu_i^{//}$	Imaginary Part of Initial Permeability	-
H	Applied magnetic field	A/m
B	Magnetic induction	T